

Chemical freeze-outs of strange and non-strange particles and residual chemical non-equilibrium

K. A. Bugaev¹, D. R. Oliinychenko^{1,2}, V. V. Sagun¹, A. I. Ivanytskyi¹, J. Cleymans³, E. G. Nikonov⁴ and G. M. Zinovjev¹

¹ Bogolyubov Institute for Theoretical Physics, Metrologichna str. 14^B, Kiev 03680, Ukraine

² FIAS, Goethe-University, Ruth-Moufang Str. 1, 60438 Frankfurt upon Main, Germany

³ Department of Physics, University of Cape Town, Rondebosch 7701, South Africa

⁴ Laboratory for Information Technologies, JINR, Joliot-Curie str. 6, 141980 Dubna, Russia

1 Abstract

We propose an elaborate version of the hadron resonance gas model with the combined treatment of separate chemical freeze-outs for strange and non-strange hadrons and with an additional γ_s factor which accounts for the remaining strange particle non-equilibration. Two sets of chemical freeze-outs parameters are connected by the conservation laws of entropy, baryonic charge, isospin projection and strangeness. The developed approach enables us to perform a high-quality fit of the hadron multiplicity ratios for AGS, SPS and RHIC energies with total $\chi^2/dof \simeq 1.05$. A special attention is paid to a complete description of the Strangeness Horn. A well-known \bar{p} , $\bar{\Lambda}$ and $\bar{\Xi}$ selective suppression problem is also discussed.

2 Introduction

Relativistic A+A collisions are an important source of experimental information about the QCD phase diagram and the strongly interacting matter properties. The last stage of such collisions is traditionally analyzed within the statistical approach which gives us an excellent opportunity to reveal the parameters of chemical freeze-out. This approach is based on the assumption of the thermal equilibrium existence during the last stage of reaction. Such an equilibrium can be reached due to intensive particle scattering. The stage of the system evolution when the inelastic reactions between hadrons stop is referred to as a chemical freeze-out (FO). Particle yields are determined by the parameters of FO, namely by chemical potentials and temperature. This general picture is a basis of the Hadron Resonance Gas Model (HRGM) [1] which is the most successful one in describing the hadronic yields measured in heavy-ion experiments for energies from AGS to LHC. Despite a significant success of the HRGM in the experimental data analysis there are a few unresolved problems. In general they are related to the description of hadron yields which contain (anti)strange quarks. Especially the energy dependence of K^+/π^+ and Λ/π^- ratios was out of high quality description. Excess of strange hadrons yields within the HRGM led physical community to ponder over strangeness suppression. The first receipt to resolve this problem was to introduce the strangeness suppression factor γ_s which should be fitted in order to describe the experimental data [2]. However, such an approach is not supported by any underlying physical model and the physical meaning of γ_s remains unclear [3, 4, 5, 6, 7]. In addition the strangeness suppression approach in its original form does not contain a hard-core repulsion between hadrons, while the latter is an important feature of the HRGM. A significant role of the hard-core repulsion was demonstrated once more in Refs. [5] where the global fit of hadron yield ratios was essentially improved (to $\chi^2/dof \simeq 1.2$) compared to all previous analyses.

The most advanced way to account for the hard-core repulsion between hadrons is to consider a hadron gas as a multi-component mixture of particles with different radii [5, 6, 8, 9]. Within this approach all baryons and mesons except for the kaons and the pions are endowed by the common hard-core radii R_b and R_m , respectively. At the same time the kaon and the pion radii R_K and R_π are fitted independently in order to provide the best description of K^+/π^+ ratio [5]. This is an important finding since the non-monotonic energy dependence of K^+/π^+ ratio may indicate some qualitative changes of the system properties and may serve as a signal of the deconfinement onset. This is a reason why this ratio known as the Strangeness Horn is of a special interest. Note, that the multi-component approach substantially increased the Strangeness Horn description quality, without spoiling the other ratios including Λ/π^- one. However, even this advanced approach does not reproduce the topmost point of the Strangeness Horn indicating that the data description is still not ideal. In order to resolve this problem in Ref. [6] the γ_s factor was considered as a free parameter within the HRGM with multi-component repulsion. Although the γ_s data fit improves the Strangeness Horn description quality sizably, it does not seem to be useful for the description of other hadron multiplicities [6].

Furthermore, in contrast to the claims established on the low-quality fit [10], at low energies it was found [6] that within the error bars in heavy ion collisions there is an enhancement of strangeness and not a suppression.

However, the effect of apparent strangeness non-equilibration can be more successfully explained by the hypothesis of separate chemical FO for all strange hadrons. Since all the hadrons made of u and d quarks are under thermal equilibration whereas the hadrons containing s quark are not, then it is reasonable to assume two different FOs for these two kinds of particles. Following this conclusion in Ref. [6, 7] a separate strangeness FO (SFO) was introduced. Note, that according to [6] both FO and SFO parameters are connected by the conservation laws of entropy, baryonic charge and isospin projection, while the net strangeness is explicitly set to zero at FO and at SFO. These conservation laws are crucial elements of the concept of separate SFO developed in [6] which allows one to essentially reduce the number of independent fitting parameters. Another principal element that differs the HRGM of [6] from the ideal gas treatment used in [7] is the presence of multi-component hard-core repulsion.

Using the HRGM of [6] it was possible to successfully describe all hadron multiplicities measured in A+A collisions at AGS, SPS and RHIC energies with $\chi^2/dof \simeq 1.06$. The concept of separate SFO led to a systematic improvement of all experimental data description. However, the topmost point of the Strangeness Horn again was not fitted even within the experimental error. Note, however, that the general description of K^+/π^+ ratio energy dependence was rather good except for the upper point.

Since an introduction of the γ_s factor demonstrated a remarkable description of all points of the Strangeness Horn, whereas the separate SFO led to a systematic improvement of all hadron yields description, we decided to combine these elements in order to describe an experimental data with the highest possible quality. This ambitious task is the main aim of the present paper. In addition, the problem of residual strangeness non-equilibration should also be clarified due to its importance from the academic point of view. Evidently, the best tool for such a purpose is the most successful version of the HRGM, i.e. the HRGM with the multi-component hadronic repulsion and SFO. As it will be shown below, such an approach makes it possible to describe 111 hadron yield ratios measured for 14 values of the center of mass collision energy $\sqrt{s_{NN}}$ in the interval from 2.7 GeV to 200 GeV with the highest quality ever achieved.

The paper is organized as follows. The basic features of the developed model are outlined in Section 3. In Section 4 we present and discuss the new fit of hadronic multiplicity ratios with two chemical freeze-outs and γ_s factor, while Section 5 contains our conclusions.

3 Model description

In what follows we treat a hadronic system as a multi-component Boltzmann gas of hard spheres. The effects of quantum statistics are negligible for typical temperatures of the hadronic gas whereas the hard-core repulsion between the particles significantly affects a corresponding equation of state [5, 8]. The present model is dealing with the Grand Canonical treatment. Hence a thermodynamical state of system under consideration is fixed by the volume V , the temperature T , the baryonic chemical potential μ_B , the strange chemical potential μ_S and the chemical potential of the isospin third component μ_{I3} . These parameters control the pressure p of the system. In addition they define the densities n_i^K of corresponding charges Q_i^K ($K \in \{B, S, I3\}$). Introducing the symmetric matrix of the second virial coefficients \mathcal{B} with the elements $b_{ij} = \frac{2\pi}{3}(R_i + R_j)^3$, we can obtain the parametric equation of state of the present model in a compact form

$$\frac{p}{T} = \sum_{i=1}^N \xi_i, \quad n_i^K = \frac{Q_i^K \xi_i}{1 + \frac{\xi^T \mathcal{B} \xi}{\sum_{j=1}^N \xi_j}}, \quad \xi = \begin{pmatrix} \xi_1 \\ \xi_2 \\ \dots \\ \xi_N \end{pmatrix}. \quad (1)$$

The equation of state is written in terms of the solutions ξ_i of the following system

$$\xi_i = \phi_i(T) \exp \left[\frac{\mu_i}{T} - \sum_{j=1}^N 2\xi_j b_{ij} + \xi^T \mathcal{B} \xi \left[\sum_{j=1}^N \xi_j \right]^{-1} \right], \quad (2)$$

$$\phi_i(T) = \frac{g_i}{(2\pi)^3} \int \exp \left(-\frac{\sqrt{k^2 + m_i^2}}{T} \right) d^3k. \quad (3)$$

It is worth to note, that quantities $T\xi_i$ have a meaning of i^{th} sort of hadrons partial pressure. Each i^{th} sort is characterized by its full chemical potential $\mu_i = Q_i^B \mu_B + Q_i^S \mu_S + Q_i^{I3} \mu_{I3}$, mass m_i and degeneracy g_i . Function $\phi_i(T)$ denotes the corresponding particle thermal density in case of ideal gas. Finally, the superscript T here is the symbolic notation for operation of a column transposition which yields a row of quantities ξ_i . The obtained model parameters for two freeze-outs and their dependence on the collision energy are shown in Figs. 1-3.

In order to account for the possible strangeness non-equilibration we introduce the γ_s factor in a conventional way by replacing ϕ_i in Eq. (2) as

$$\phi_i(T) \rightarrow \phi_i(T)\gamma_s^{s_i}, \quad (4)$$

where s_i is a number of strange valence quarks plus number of strange valence anti-quarks.

The principal difference of the present model from the traditional approaches is that we employ an independent chemical FO of strange particles. Let us consider this in some detail. The independent freeze-out of strangeness means that inelastic reactions (except for the decays) with hadrons made of s quarks are switched off at the temperature T_{SFO} , the baryonic chemical potential μ_{BSFO} , the strange chemical potential μ_{SSFO} , the isospin third projection chemical potential μ_{I3SFO} and the three-dimensional emission volume V_{SFO} . In general case these parameters of SFO do not coincide with the temperature T_{SFO} , the chemical potentials μ_{BSFO} , μ_{SSFO} , μ_{I3SFO} and the volume V_{SFO} which characterize the freeze-out of non-strange hadrons. The particle yields are given by the charge density n_i^K in (1) and the corresponding volume at FO and at SFO.

At the first glance a model with independent SFO contains four extra fitting parameters for each energy value compared to the traditional approach (temperature, three chemical potentials and the volume at SFO instead of strangeness suppression/enhancement factor γ_s). However, this is not the case due to the conservation laws. Indeed, since the entropy, the baryonic charge and the isospin third projection are conserved, then the parameters of FO and SFO are connected by the following equations

$$s_{FO}V_{FO} = s_{SFO}V_{SFO}, \quad (5)$$

$$n_{FO}^B V_{FO} = n_{SFO}^B V_{SFO}, \quad (6)$$

$$n_{FO}^{I3} V_{FO} = n_{SFO}^{I3} V_{SFO}. \quad (7)$$

The effective volumes can be excluded, if these equations are rewritten as

$$\left. \frac{s}{n^B} \right|_{FO} = \left. \frac{s}{n^B} \right|_{SFO}, \quad \left. \frac{n^B}{n^{I3}} \right|_{FO} = \left. \frac{n^B}{n^{I3}} \right|_{SFO}. \quad (8)$$

Thus, the baryonic μ_{BSFO} and the isospin third projection μ_{I3SFO} chemical potentials at SFO are now defined by Eqs. (8). Note, that the strange chemical potentials μ_{SFO} and μ_{SSFO} are found from the condition of vanishing net strangeness at FO and SFO, respectively. Therefore, the concept of independent SFO leads to an appearance of one independently fitting parameter T_{SFO} . Hence, the independent fitting parameters are the following: the baryonic chemical potential μ_B , the chemical potential of the third projection of isospin μ_{I3} , the chemical freeze-out temperature for strange hadrons T_{SFO} , the chemical freeze-out temperature for all non-strange hadrons T_{FO} and the γ_s factor.

An inclusion of the width Γ_i of hadronic states is an important element of the present model. It is due to the fact that the thermodynamical properties of the hadronic system are sensitive to the width [5, 6, 11]. In order to account for the finite width of resonances we perform the usual modification of the thermal particle density ϕ_i . Namely, we convolute the Boltzmann exponent under the integral over momentum with the normalized Breit-Wigner mass distribution. As a result, the modified thermal particle density of i^{th} sort hadron acquires the form

$$\int \exp\left(-\frac{\sqrt{k^2 + m_i^2}}{T}\right) d^3k \rightarrow \frac{\int_{M_0}^{\infty} \frac{dx}{(x-m_i)^2 + \Gamma_i^2/4} \int \exp\left(-\frac{\sqrt{k^2 + x^2}}{T}\right) d^3k}{\int_{M_0}^{\infty} \frac{dx}{(x-m_i)^2 + \Gamma_i^2/4}}. \quad (9)$$

Here m_i denotes the mean mass of hadron and M_0 stands for the threshold in the dominant decay channel. The main advantages of this approximation is a simplicity of its realization and a clear way to account for the finite width of hadrons.

The observed hadronic multiplicities contain the thermal and decay contributions. For example, a large part of pions is produced by the decays of heavier hadrons. Therefore, the total multiplicity is obtained as a sum of thermal and decay multiplicities, exactly as it is done in a conventional model. However, writing the formula for final particle densities, we have to take into account that volumes of FO and SFO can be different:

$$\frac{N^{fin}(X)}{V_{FO}} = \sum_{Y \in FO} BR(Y \rightarrow X) n^{th}(Y) + \sum_{Y \in SFO} BR(Y \rightarrow X) n^{th}(Y) \frac{V_{SFO}}{V_{FO}}. \quad (10)$$

Here the first term on the right hand side is due to decays after FO whereas the second one accounts for the strange resonances decayed after SFO. The factor V_{SFO}/V_{FO} can be replaced by n_{FO}^B/n_{SFO}^B due to baryonic charge conservation. $BR(Y \rightarrow X)$ denotes the branching ratio of the Y-th hadron decay into the X-th hadron, with the definition $BR(X \rightarrow X) = 1$ used for the sake of convenience. The input parameters of the present model (masses m_i , widths Γ_i , degeneracies g_i and branching ratios of all strong decays) were taken from the particle tables of the thermodynamical code THERMUS [12].

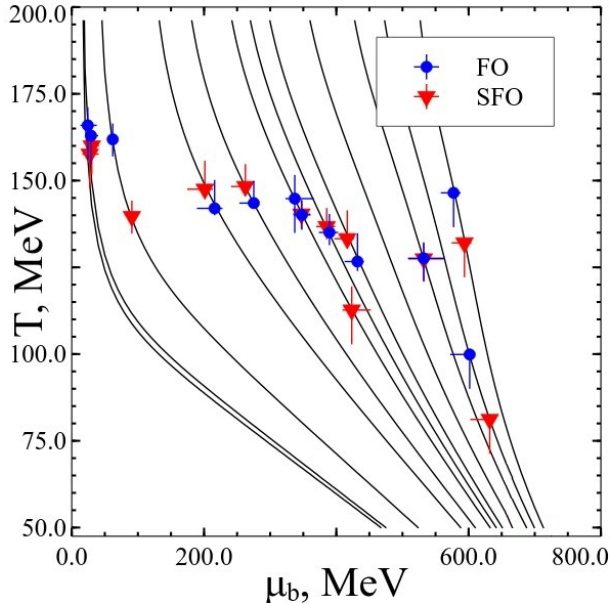


Figure 1: (Colour on-line) Chemical freeze-outs parameters in the model with two freeze-outs and with the γ_s fit. Baryonic chemical potential dependence of the chemical freeze-out temperature for SFO (marked with triangles) and for FO (marked with circles). The solid black curves correspond to the isentropes $s/\rho_B = \text{const}$, on which the FO and the SFO points are located.

4 Results

Data sets and fit procedure. The present model is applied to fit the data. We take the ratios of particle multiplicities at midrapidity as the data points. In contrast to fitting multiplicities themselves such an approach allows us to cancel the possible experimental biases. In this paper we use the data set almost identical to Ref. [6]. At the AGS energies ($\sqrt{s_{NN}} = 2.7 - 4.9$ AGeV or $E_{lab} = 2 - 10.7$ AGeV) the data are available with a good energy resolution above 2 AGeV. However, for the beam energies 2, 4, 6 and 8 AGeV only a few data points are available. They corresponds to the yields for pions [13, 14], for protons [15, 16], for kaons [14] (expect for 2 AGeV). The integrated over 4π data are also available for Λ hyperons [17] and for Ξ^- hyperons (for 6 AGeV only) [18]. However, as was argued in Ref. [3], the data for Λ and Ξ^- should be recalculated for midrapidity. Therefore, instead of raw experimental data we used the corrected values from [3]. Next comes the data set at the highest AGS energy ($\sqrt{s_{NN}} = 4.9$ AGeV or $E_{lab} = 10.7$ AGeV). Similarly to [5], here we analyzed only the NA49 mid-rapidity data [19, 20, 21, 22, 23, 24]. Since the RHIC high energy data of different collaborations agree with each other, we analyzed the STAR results for $\sqrt{s_{NN}} = 9.2$ GeV [25], $\sqrt{s_{NN}} = 62.4$ GeV [26], $\sqrt{s_{NN}} = 130$ GeV [27, 28, 29, 30] and 200 GeV [30, 31, 32].

The criterion to define the fitting parameters of the present model is a minimization of $\chi^2 = \sum_i \frac{(r_i^{theor} - r_i^{exp})^2}{\sigma_i^2}$, where r_i^{theor} and r_i^{exp} are, respectively, the theoretical and the experimental values of particle yields ratios, σ_i stands for the corresponding experimental error and a summation is performed over all available experimental points.

Combined fit with SFO and γ_s factor. Recently performed comprehensive data analysis [6] for two alternative approaches, i.e the first one with γ_s as a free parameter and the second one with separate FO and SFO, showed the advantages and disadvantages of both methods. Thus, the γ_s fit provides one with an opportunity to noticeably improve the Strangeness Horn description with $\chi^2/dof = 3.3/14$, comparably to the previous result $\chi^2/dof = 7.5/14$ [5], but there are only slight improvements of the ratios with strange baryons (global $\chi^2/dof : 1.16 \rightarrow 1.15$). The obtained results for the SFO approach demonstrate a nice fit quality for the most problematic ratios for the HRGM, especially for \bar{p}/π^- , $\bar{\Lambda}/\Lambda$, $\bar{\Xi}^-/\Xi^-$ and $\bar{\Omega}/\Omega$. Although the overall $\chi^2/dof \simeq 1.06$ is notably better than with the γ_s factor [5, 6], but the highest point fitting of the Horn got worse. These results led us to an idea to investigate the combination of these two approaches in order to get the high-quality Strangeness Horn description without spoiling the quality of other particle ratios.

For 14 values of collision energy $\sqrt{s_{NN}} = 2.7, 3.3, 3.8, 4.3, 4.9, 6.3, 7.6, 8.8, 9.2, 12, 17, 62.4, 130, 200$ GeV the best description with two separate freeze-outs and the γ_s fit gives $\chi^2/dof = 42.96/41 \simeq 1.05$, which is only a very slight improvement compared to the previously obtained results $\chi^2/dof = 58.5/55 \simeq 1.06$ found for two freeze-outs (strange and all other particles), which are connected by the conservation laws. Note, however, that the value of χ^2 itself, not divided by number of degrees of freedom, has improved notably, although the

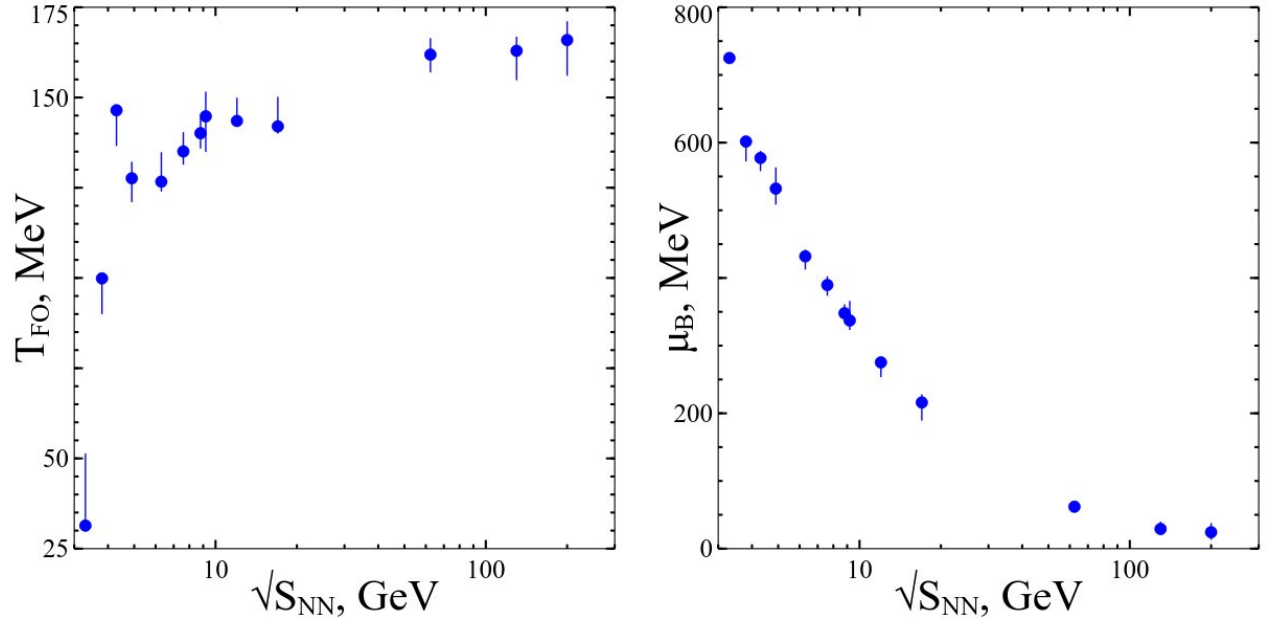


Figure 2: (Colour on-line) The behavior of the model parameters: chemical freeze-out temperature T vs. $\sqrt{s_{NN}}$ (left panel) and the freeze-out baryonic chemical potential μ_B vs. $\sqrt{s_{NN}}$ (right panel).

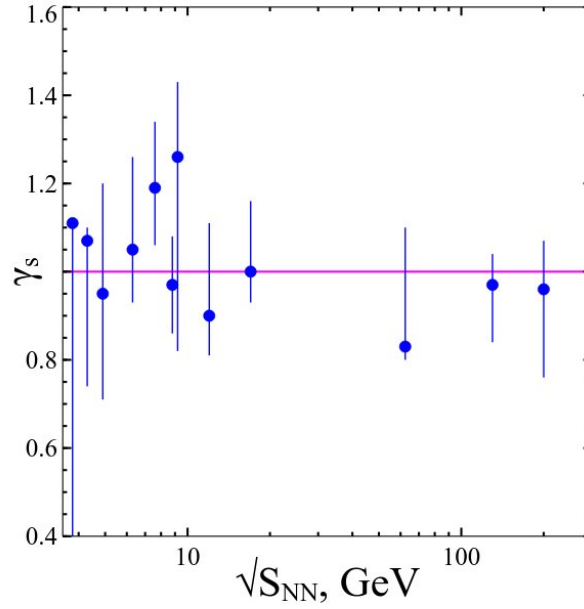


Figure 3: (Colour on-line) $\sqrt{s_{NN}}$ dependence of the γ_s factor in the model with two freeze-outs and the γ_s fit.

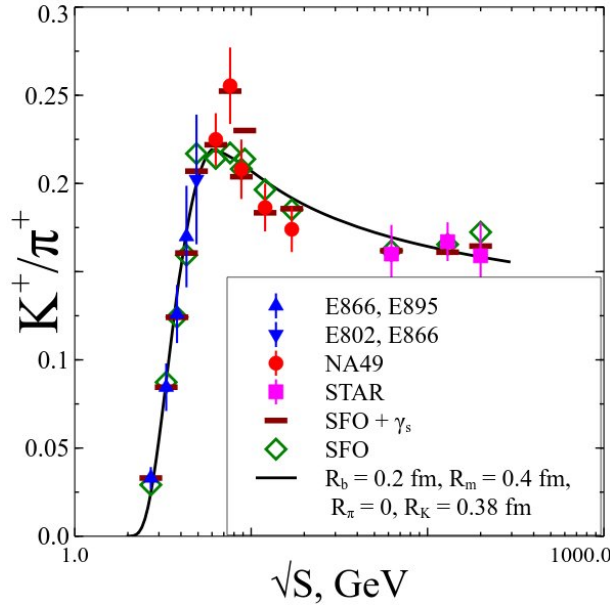


Figure 4: (Colour on-line) $\sqrt{s_{NN}}$ dependences of K^+/π^+ ratio. The solid line corresponds to the results of [5]. Horizontal bars correspond to the present model with SFO+ γ_s fit, while the diamonds correspond to the results previously obtained for SFO [6].

deviation of the γ_s factor from 1 does not exceed 27 % (see Fig. 3). These findings motivate us to study what ratios and at what energies are improved.

As we mentioned earlier, at each collision energy there are five independent fitting parameters in the considered model with the simultaneous SFO and the γ_s fit, while for some collision energies the number of experimental ratios is lower or equal to the number of parameters. For example, for the energies $\sqrt{s_{NN}} = 2.7, 3.3, 3.8, 4.3, 9.2, 62.4$ GeV the number of available ratios is small (4, 5, 5, 5, 5, 5, respectively) from which only kaons and Λ contain strange quarks. Therefore, for these energies we obtained a perfect data description since we had to solve the above equations. As a result for these energies the relative deviation of the fit is almost a zero, but it gives us somewhat larger uncertainties for the fitting parameters.

For the energies $\sqrt{s_{NN}} = 17, 130$ GeV we observed that the resulting fit quality became better compared to the work [6]. The most significant improvements correspond to the collision energies $\sqrt{s_{NN}} = 6.3, 7.6$, and 12 GeV, that are plotted in Fig. 5. Fig. 5 demonstrates very nice fit quality, especially for such traditionally problematic ratios as K^+/π^+ , π^-/π^+ , $\bar{\Lambda}/\pi^-$ and φ/K^+ . For $\sqrt{s_{NN}} = 7.6$ GeV the seven ratios out of ten are improved.

A special attention in our consideration was paid to the Strangeness Horn, i.e. to K^+/π^+ ratio. Another reason for a thorough study of the Strangeness Horn is a traditional problem of the HRGM to fit it. As one can see from Fig. 4, the remarkable K^+/π^+ fit improvement for $\sqrt{s_{NN}} = 2.7, 3.3, 4.3, 4.9, 6.3, 7.6, 12$ GeV justifies the usage of the present model. Quantitatively, we found that χ^2/dof improvement due to SFO+ γ_s introduction is $\chi^2/dof = 1.5/14$, i.e. even better than it was done in [6] with $\chi^2/dof = 3.3/14$ for the γ_s fitting approach and $\chi^2/dof = 6.3/14$ for SFO and $\gamma_s = 1$.

In addition, in Fig. 6 we give the Λ/π^- and $\bar{\Lambda}/\pi^-$ ratios to show that two separate freeze-outs inclusion with the γ_s fit still does not improve these ratios. The Λ/π^- fit quality, for instance, is ($\chi^2/dof = 10/8$). Hence, up to now the best fit of the Λ/π^- ratio was obtained within the SFO approach with $\gamma_s = 1$. As it was mentioned in [3, 4, 5] a too slow decrease of model results for Λ/π^- ratio compared to the experimental data is typical for almost all statistical models. Evidently, the too steep rise in Λ/π^- behavior is a consequence of the $\bar{\Lambda}$ anomaly [3, 33]. Similar results are reported in Refs. [34, 35, 36] as the \bar{p} , $\bar{\Lambda}$ and $\bar{\Xi}$ selective suppression. Since even an introduction of the separate strangeness freeze-out with the strangeness enhancement factor does not allow us to better describe these ratios, we believe that there is an unclarified physical reason which is responsible for it.

Within the present model we also found a selective improvement and a certain degradation of the fit quality of various ratios for different collision energies. For instance, the π^-/π^+ ratio is slightly increased for $\sqrt{s_{NN}} = 6.3$ and 7.6 GeV, but the situation drastically changes for $\sqrt{s_{NN}} = 12$ GeV. The same tendency is typical for \bar{p}/p . On the contrary, for $\bar{\Xi}^-/\Lambda$ ratio there is a noticeably worse data description within SFO+ γ_s approach at $\sqrt{s_{NN}} = 6.3, 7.6$ GeV, but for $\sqrt{s_{NN}} = 12$ GeV the fit quality is sizably better compared to all previous approaches. Thus, within the present model we reveal a noticeable change in the trend of some ratios at $\sqrt{s_{NN}} = 7.6-12$ GeV.

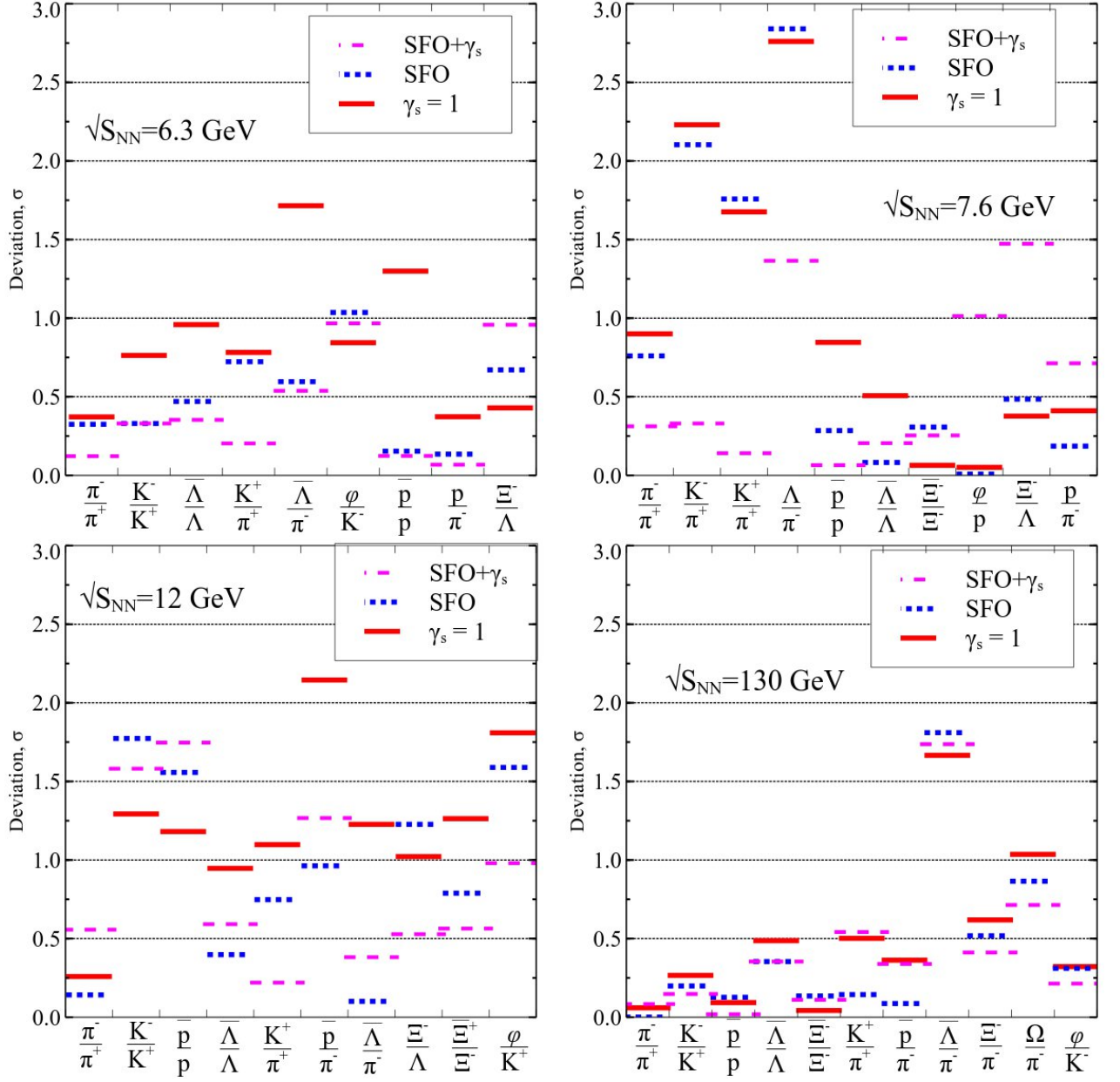


Figure 5: (Colour on-line) Relative deviation of the theoretical description of ratios from the experimental value in units of the experimental error σ . Particle ratios vs. the modulus of relative deviation ($\frac{|r^{theor}-r^{exp}|}{\sigma^{exp}}$) for $\sqrt{s_{NN}} = 6.3, 7.6, 12$ and 130 GeV are shown. Solid lines correspond to the model with a single FO of all hadrons and $\gamma_s = 1$, blue dotted lines correspond to the model with SFO. The results of a model with a combined fit with SFO and γ_s are highlighted by magenta dashed lines.

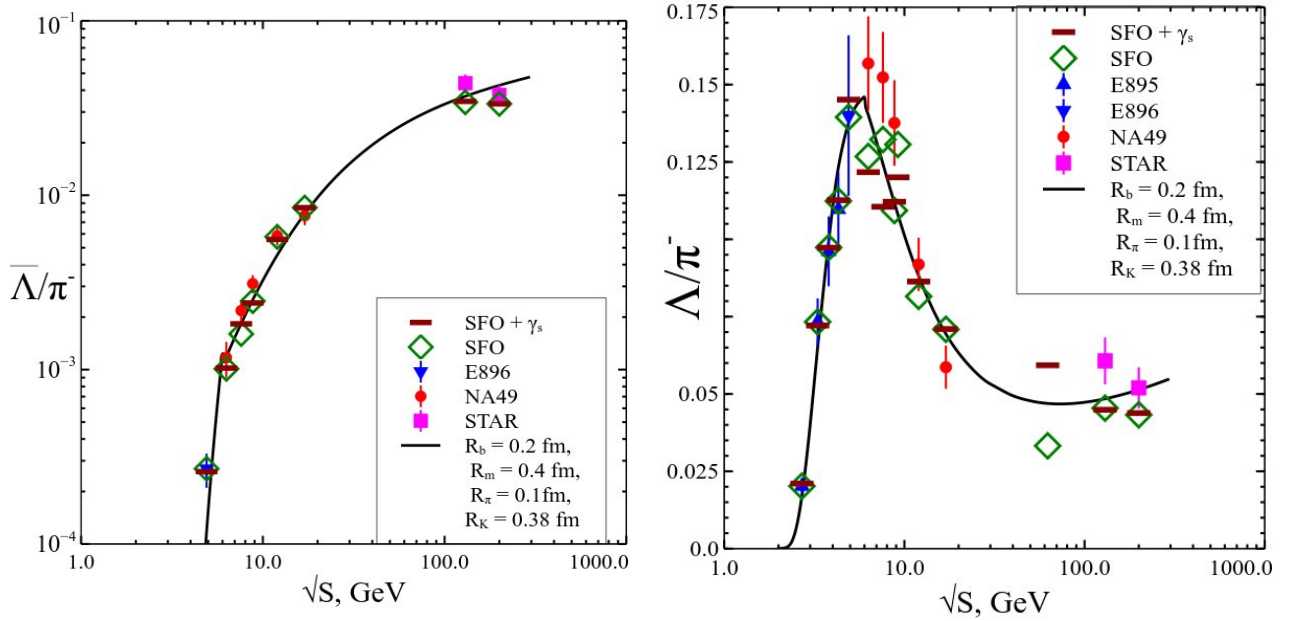


Figure 6: (Colour on-line) $\sqrt{s_{NN}}$ dependences of $\bar{\Lambda}/\pi^-$ (left panel) and Λ/π^- (right panel) ratios. The solid line correspond to the results of [5]. Horizontal bars correspond to SFO+ γ_s model, while green diamonds correspond to the previously obtained results for the SFO model [6].

5 Conclusions

We have performed an elaborate fit of the data measured at AGS, SPS and RHIC energies within the multi-component hadron resonance gas model. The suggested approach to separately treat the freeze-outs of strange and non-strange hadrons with the simultaneous γ_s fitting gives rise for the top-notch Strangeness Horn description with $\chi^2/dof=1.5/14$. The developed model clearly demonstrates that the successful fit of hadronic multiplicities includes all the advantages of these two approaches discussed in [6]. As a result for $\sqrt{s_{NN}} = 6.3, 7.6, 12, 130$ GeV we found a significant data fit quality improvement. The achieved total value of χ^2/dof is $42.96/41 \simeq 1.05$, while the γ_s values are consistent with the conclusion $\gamma_s \simeq 1$ (within the error bars). A possible exception is the topmost point of the Strangeness Horn, at which the mean value of the strangeness enhancement factor is $\gamma_s \simeq 1.27$, but with the large error bars. In addition, the description of ratios containing the non-strange particles, especially such as π^-/π^+ and \bar{p}/p , gets better compared to previously reported results [5, 6]. At the same time the lack of available data at $\sqrt{s_{NN}} = 2.7, 3.3, 3.8, 4.3, 9.2, 62.4$ GeV forced us to solve the corresponding equations which in combination with the large experimental error bars led to rather large uncertainties of the fitting parameters.

From a significant improvement of the data description we conclude that the concept of separate chemical freeze-out of strange particles is an essential part of heavy ion collision phenomenology which should be taken into account in further studies of strongly interacting matter properties. However, the remaining problem with \bar{p} , $\bar{\Lambda}$, Ξ ratios led us to a conclusion that there is an unclarified physical reason which is responsible for them. The residual non-equilibration of strange particles found here seems to be weak and, perhaps, the better experimental data will help us to reduce it further.

The obtained description of the hadron multiplicity ratios reached the highest quality ever achieved and this fact demonstrates that the suggested approach is almost a precise tool to elucidate the thermodynamics properties of hadron matter at two chemical freeze-outs. The fresh illustrations to this statement can be found in [11]. However, to get more reliable conclusions from this approach we need more experimental data with an essentially higher accuracy.

Acknowledgments. We would like to thank A. Andronic for providing an access to well-structured experimental data. The authors are thankful to I. N. Mishustin, D. H. Rischke and L. M. Satarov for valuable comments. K.A.B., A.I.I. and G.M.Z. acknowledge a support of the Fundamental Research State Fund of Ukraine, Project No F58/04. K.A.B. acknowledges also a partial support provided by the Helmholtz International Center for FAIR within the framework of the LOEWE program launched by the State of Hesse.

References

- [1] Braun-Munzinger P., Redlich K. and Stachel J., In *Hwa, R.C. (ed.) *et al.*: Quark gluon plasma***13** (2003) 491.
- [2] Rafelsky J., Phys. Lett. B **62** (1991) 333.
- [3] Andronic A., Braun-Munzinger P. and Stachel J., Nucl. Phys. A **772** (2006) 167 and references therein.
- [4] Andronic A., Braun-Munzinger P. and Stachel J., Phys. Lett. B **673** (2009) 142.
- [5] Bugaev K. A., Oliinychenko D. R., Sorin A. S. and Zinovjev G. M., Eur. Phys. J. A **49** (2013)30–1-8 and references therein.
- [6] Bugaev K.A. *et al.*, Europhys. Lett. **104** (2013) 22002.
- [7] Chatterjee S., Godbole R. M. and Gupta S., Phys. Lett. B **727** (2013) 554.
- [8] Zeeb G., Bugaev K. A., Reuter P. T. and Stöcker H. Ukr. J. Phys. **53** (2008) 279.
- [9] Oliinychenko D. R. , BugaevK. A. and Sorin A. S., Ukr. J. Phys. **58** (2013) 211.
- [10] Becattini F., Manninen J. and Gazdzicki M., Phys. Rev. C **73** (2006) 044905.
- [11] Bugaev K. A., Ivanytskyi A. I., Oliinychenko D.R., Nikonov E. G., Sagun V. V. and Zinovjev G. M., arXiv:1311.4367 [nucl-th].
- [12] Wheaton S., Cleymans J. and Hauer M., Comput. Phys. Commun. **180** (2009) 84.
- [13] Klay J. L. *et al.*, Phys. Rev. C **68** (2003) 054905.
- [14] Ahle L. *et al.*, Phys. Lett. B **476** (2000) 1.
- [15] Back B. B. *et al.*, Phys. Rev. Lett. **86** (2001) 1970.
- [16] Klay J. L. *et al.*, Phys. Rev. Lett. **88** (2002) 102301.
- [17] Pinkenburg C. *et al.*, Nucl. Phys. A **698** (2002) 495c.
- [18] Chung P. *et al.*, Phys. Rev. Lett. **91** (2003) 202301.
- [19] Afanasiev S. V. *et al.*, Phys. Rev. C **66** (2002) 054902.
- [20] Afanasiev S. V. *et al.*, Phys. Rev. C **69** (2004) 024902.
- [21] Anticic T. *et al.*, Phys. Rev. Lett. **93** (2004) 022302.
- [22] Afanasiev S. V. *et al.*, Phys. Lett. B **538** (2002) 275.
- [23] Alt C. *et al.*, Phys. Rev. Lett. **94** (2005) 192301.
- [24] Afanasiev S. V. *et al.*, Phys. Lett. B **491** (2000) 59.
- [25] Abelev B. *et al.*, Phys. Rev. C **81** (2010) 024911.
- [26] Abelev B. *et al.*, Phys. Rev. C **79** (2009) 034909.
- [27] Adams J. *et al.*, Phys. Rev. Lett. **92** (2004) 182301.
- [28] Adams J. *et al.*, Phys. Lett. B **567** (2003) 167.
- [29] Adler C. *et al.*, Phys. Rev. C **65** (2002) 041901(R).
- [30] Adams J. *et al.*, Phys. Rev. Lett. **92** (2004) 112301.
- [31] Adams J. *et al.*, Phys. Lett. B **612** (2005) 181.
- [32] Billmeier A. *et al.*, J. Phys. G **30** (2004) S363.
- [33] Back B. B. *et al.*, Phys. Rev. Lett. **87** (2001) 242301.
- [34] Becattini F. *et al.*, Phys. Rev. C **85** (2012) 044921.
- [35] Becattini F. *et al.*, Phys. Rev. Lett. **111** (2013) 082302.
- [36] Stachel J., Andronic A., Braun-Munzinger P. and Redlich K., arXiv:1311.4662 [nucl-th].